Residues from Transmembrane Helices 3 and 5 Participate in Leukotriene B_4 Binding to BLT_1[†]

Alan Sabirsh,*[,‡] Robert P. Bywater,[§] Jesper Bristulf,[||] Christer Owman,[||] and Jesper Z. Haeggström[‡]

Department of Medical Biochemistry and Biophysics, Karolinska Institutet, S-171 77 Stockholm, Sweden, Adelard Institute, London NW7 3NY, England, Magdalen College, Oxford OX1 4AU, England, and Drug Target Discovery, Lund University, BMC A12, 22184 Lund, Sweden

Received January 13, 2006; Revised Manuscript Received March 1, 2006

ABSTRACT: Leukotrienes are inflammatory mediators that bind to seven transmembrane, G-protein-coupled receptors (GPCRs). Here we examine residues from transmembrane helices 3 and 5 of the leukotriene B_4 (LTB_4) receptor BLT_1 to elucidate how these residues are involved in ligand binding. We have selected these residues on the basis of (1) amino acid sequence analysis, (2) receptor binding and activation studies with a variety of leukotriene-like ligands and recombinant BLT_1 receptors, (3) previously published recombinant BLT_1 mutants, and (4) a computed model of the active structure of the BLT_1 receptor. We propose that LTB_4 binds with the polar carboxylate group of LTB_4 near the extracellular surface of BLT_1 and with the hydrophobic LTB_4 tail pointing into the transmembrane regions of the receptor protein. The carboxylate group and the two hydroxyls of LTB_4 interact with Arg178 and Glu185 in transmembrane helix 5. Residues from transmembrane helix 3, Val105 and Ile108, also line the pocket deeper inside the receptor. LTB_4 is becoming increasingly important as an immunomodulator during a number of pathologies, including atherosclerosis. Detailed information about the LTB_4 binding mechanism, and the receptor residues involved, will hopefully aid in the design of new immunomodulatory drugs.

The leukotrienes are a family of eicosanoid lipid mediators derived from the oxidative metabolism of arachidonic acid. These proinflammatory substances are important for normal host defense, as well as the pathophysiology of a number of inflammatory and allergic diseases, especially in the skin joints, circulatory system, and respiratory tract (e.g., refs *1*−*4*). The present work focuses on the heptahelical G-protein-coupled receptor (GPCR)[1] BLT_1, the primary receptor for leukotriene B_4 (LTB_4).

There is relatively little mutational data available for the portions of the BLT_1 receptor that are likely to be involved in ligand binding. Chiang et al. (*5*) studied chimeric receptors constructed by exchanging successive portions of BLT_1 for the corresponding portions of the lipoxin A_4 receptor ALXR. This study indicated that LTB_4 binding is affected by changes made anywhere in BLT_1, with the exception of the C-terminal tail, but receptor protein expression at the cell surface was not examined in this study. Gearing et al. (*6*) have produced an epitope-tagged chimeric protein consisting of the extracellular half of BLT_1 and the intracellular half of the purine receptor, P2Y2. These receptors were well expressed, bound LTB_4 at least as well as wild-type receptors, and were functionally similar to the wild-type BLT_1. This implies that the essential LTB_4 binding epitopes are located within the upper (extracellular) half of the protein or involve amino acids that are similar in both receptors. Finally, an elegant pair of studies published by Banères et al. (*7*, *8*) examined solubilized BLT_1 receptors produced using *Escherichia coli* bacteria. These studies showed that each BLT_1 receptor binds one LTB_4 molecule and that both the ligand and the receptor undergo conformational changes during ligand binding.

The purpose of the present work is to use point mutations to elucidate which BLT_1 residues are important for LTB_4 binding. No crystallographic structure data exist for BLT_1, so in order to make informed decisions about which residues to mutate, we began with the construction of a homology model of BLT_1 based on the structure of bovine rhodopsin, the only GPCR for which detailed structural data are currently available (*9*). The implausible results obtained from preliminary docking experiments with this BLT_1 model suggested that an active conformation of the receptor would be necessary for exploring the binding of agonists. We have therefore used an active, theoretical, rhodopsin conformation as a modeling template for BLT_1 (*10*). A theoretical model of an active rhodopsin conformation is not, however, an entirely appropriate template for BLT_1 because the activation of rhodopsin receptors probably induces protein conformations that are unique to these receptors. To avoid this problem, we then docked LTB_4 into the active BLT_1 receptor

[†] This study was financially supported by the AFA Health Foundation, the Swedish Medical Research Council (03X-10350), Konung Gustav V:s 80 årsfond, and EC FP6 funding (LSHM-CT-2004-005033). This publication reflects only the author's views. The European Commission is not liable for any use that may be made of information herein.

* Corresponding author. E-mail: Alan.Sabirsh@ki.se. Tel: +46 (0)8 524 876 30. Fax: +46 (0)8 736 04 39.

[‡] Karolinska Institutet.

[§] Adelard Institute and Magdalen College.

[||] Lund University.

[1] Abbreviations: GPCR, heptahelical G-protein-coupled receptor; LT, leukotriene; BLT_1 and BLT_2, LTB_4 receptors 1 and 2; HETE, hydroxyeicosatetraenoic acid; TMx, receptor transmembrane α helix, where the "x" refers to helix 1−7; WT, wild type; EGFP, enhanced green fluorescent protein.

10.1021/bi060076t CCC: $33.50
Published on Web 04/12/2006

model and identified several residues as candidates for biochemical validation using point mutations, together with binding and functional assays. Here we present the interaction of residues from TMs 3 and 5 with LTB_4 and several other ligands. We have used these results, together with previously published mutational data, to create the first proposal for LTB_4 binding to its principal receptor, BLT_1.

EXPERIMENTAL PROCEDURES

Chemicals and Reagents. 6-*trans*-LTB_4 (5*S*,12*R*-dihydroxy-6,8,10-*trans*-14-*cis*-eicosatetraenoic acid), 6-*trans*-12-*epi*-LTB_4 (5*S*,12*S*-dihydroxy-6,8,10-*trans*-14-*cis*-eicosatetraenoic acid), and 6-*trans*-8-*cis*-LTB_4 (5*S*,12*R*-dihydroxy-6,10-*trans*-8,14-*cis*-eicosatetraenoic acid) were biosynthesized from incubations of recombinant mutated Tyr378Phe LTA_4 hydrolase (*11*) with synthetic LTA_4, prepared as described (*12*). Each compound was purified and isolated on reverse-phase HPLC, as described (*13*). After evaporation of the HPLC mobile phase under N_2, the compounds were dissolved in methanol and stored at −80 °C in light-protected vials.

The following compounds were obtained from BIOMOL Research Laboratories (Plymouth Meeting, PA): LTB_5 (leukotriene B_5, 5*S*,12*R*-dihydroxy-6,14,17-*cis*-8,10-*trans*-eicosatetraenoic acid), LTB_3 (leukotriene B_3, 5*S*,12*R*-dihydroxy-6-*cis*-8,10-*trans*-eicosatetraenoic acid), 5*S*,12*S*-diHETE (5*S*,12*S*-dihydroxy-6,10-*trans*-8,14-*cis*-eicosatetraenoic acid), 15*S*-HETE (15*S*-hydroxy-5,8,11-*cis*-13-*trans*-eicosatetraenoic acid), 20-COOH-LTB_4 (20-carboxyleukotriene B_4), 20-OH-LTB_4 (20-hydroxyleukotriene B_4), 5*S*-HETE (5*S*-hydroxy-6-*cis*-8,11,14-*trans*-eicosatetraenoic acid), 12*R*-HETE (12*R*-hydroxy-5,8,14-*cis*-10-*trans*-eicosatetraenoic acid), and 12*S*-HETE (12*S*-hydroxy-5,8,14-*cis*-10-*trans*-eicosatetraenoic acid).

Quantification of all compounds was carried out by UV spectrophotometry using extinction coefficients of 23000 (at 236 nm) for hydroxyeicosatetraenoic acids (HETEs), 40000 (at 269 and 268 nm) for 6-*trans*-8-*cis*-LTB_4 and 5*S*,12*S*-diHETE, 50000 (at 270 nm) for LTB_4, 20-OH-LTB_4, 20-COOH-LTB_4, LTB_3, and LTB_5, and 50000 (at 268 nm) for 6-*trans*-LTB_4 and 6-*trans*-12-*epi*-LTB_4. The substances were >99% pure, with the exception of 5*S*,12*S*-diHETE (>90%), 6-*trans*-LTB_4 (>75%), and 6-*trans*-8-*cis*-LTB_4 (>94%). Tritiated LTB_4 (195 Ci/mmol) was from NEN Life Science Products (Boston, MA) or International Isotopes Clearing House Inc. (Leawood, KS). All tissue culture media and reagents were from Life Technologies (Täby, Sweden).

Alexa Fluor 568 (Molecular Probes) was added to LTB_4-APA (LTB_4 aminopropylamine; BIOMOL) according to Sabirsh et al. (*14*) to produce fluorescent LTB_4 (LTB_4-568).

Cell Culture. Cultures of HeLa HF1 luciferase reporter cells were created and maintained according to Kotarsky et al. (*15*). HF1p sham cells and HF1 cells expressing wild-type, untagged, BLT_1 receptors (HF1pBLT_1), EGFP-tagged BLT_1 (HF1pBLT_1-EGFP), or one of nine point mutations of the wild-type receptor (e.g., Arg178Glu) were created by transfecting cells with plasmid DNAs using Lipofectamine PLUS (Invitrogen) as described by the manufacturer, and stable receptor-expressing clones were selected using puromycin.

BLT_1 Point Mutations. All of the mutations were generated using QuickChange (Stratagene) according to the manufacturer's recommendations except that Platinum Pfx DNA polymerase (Invitrogen) was used instead of Pfu Turbo DNA polymerase. The template for the generation of BLT_1 mutants was the pEAK-BLT1-HFTE vector containing a human BLT_1 receptor that has been C-terminally tagged with a His_{10} tag (H), a FLAG tag (F), and the recognition site for the tobacco etch virus (T) protease followed by EGFP (E). Two complementary primers containing the desired base pair changes in the middle of a minimum of 34 bases of wild-type sequence were used as primers for each mutation. PCR products were generated according to the manufacturer's recommendations, purified using G-50 gel filtration spin columns (Amersham), and treated with 20 units of *Dpn*I (New England Biolabs) before they were used to transform competent *E. coli* XL-1 Blue cells (Stratagene). Bacterial colonies were screened using PCR and mutant-specific primers. Plasmids, prepared from positive clones, were purified using QIAspin Miniprep columns (Qiagen), and plasmid integrity was confirmed using automated DNA sequencing with BigDye (Applied Biosystems).

Flow Cytometry. Flow cytometric analysis of receptor expression was performed as previously described (*16*). Red fluorescent anti-BLT_1 antibody (14F11) was obtained from R and D Systems. This antibody does not activate BLT_1 and has been shown to bind epitopes that are unrelated to the LTB_4 binding site but which are dependent on the tertiary structure of the receptor protein (*16*).

Membrane Preparation. Using methods previously described (*16*), membranes were prepared from monoclonal HF1 cell lines, each expressing one BLT_1 construct. Polymorphonuclear cells (PMNCs) were isolated from human buffy coats, following red cell sedimentation with 0.6% dextran, using a density gradient (Lymphoprep; Axis Shield, Olsa, Norway) centrifugation. Essentially pure and viable PMNCs (>95%, verified histologically using cellular morphology, >99% viable using trypan blue exclusion) were obtained following washing, and these cells were homogenized as above.

Binding Assays. Radioligand binding assays were performed using opaque white 96-well filter plates with FC glass fiber filters (model MAFC-NOB, multiscreen assay system; Millipore, Bedford, MA). The plates were presoaked with binding buffer (0.02 M HEPES, 10 mM $CaCl_2$, 10 mM $MgCl_2 \cdot 6H_2O$, pH 7.5), which was then exchanged for 75 μL of binding buffer containing 1.0 nM ^{3}H-LTB_4 and, if necessary, 2.0 μM unlabeled LTB_4 in order to determine nonspecific binding. The binding reaction was started by adding another 75 μL of binding buffer containing 1.0 μg of rehomogenized cell membrane and the appropriate concentration of any test substance. For experiments with LTC_4 and LTD_4 the binding buffer also contained a final concentration of 50 mM serine−borate or 20 mM L-penicillamine, respectively. The membrane−ligand solution was incubated for 1 h at room temperature. The reaction was terminated by rapid filtration, and the filters were then washed three times with 200 μL volumes of ice-cold washing buffer (20 mM Tris base, 0.5 g/L BSA). Excess washing buffer was removed by blotting, and the plates were dried in a vacuum oven at 40 °C for 30 min. Twenty-five microliters of Microscint-O (Packard) was then added to each well, and ^{3}H-LTB_4 binding was evaluated using TopCount

NXT (Packard) and Micro Beta (Wallac) scintillation counters.

There was a linear correlation between the amount of radioligand bound and the amount of membrane protein added to each well. Counting efficiency was approximately 20%. No specific ^{3}H-LTB_4 binding to sham-transfected HF1 cells was observed.

For each ligand, the concentration that inhibited half of the ^{3}H-LTB_4 binding (IC_{50}) was determined from competitive binding curves using nonlinear regression (Graph Pad, Prism), and this in turn was used to calculate K_i according to Cheng and Prusoff (*17*). The results shown were obtained from duplicate wells in three separate experiments unless otherwise stated.

Functional Assays of BLT_1 Activity Using a Luciferase Reporter System. The assay for agonist-induced luciferase production was performed according to Kotarsky et al. (*15*). Briefly, this is an assay that was designed to funnel several GPCR signaling pathways (including calcium and MAP kinase pathways) toward a luciferase gene by using a synthetic enhancer containing nine 12-*O*-tetradecanoylphorbol 13-acetate responsive elements fused to a minimal CMV (cytomegalovirus) promoter. BLT_1 produces a large robust signal using this system. Curve fitting and statistical analysis were performed using Prism (GraphPad). To normalize the responses obtained from the reporter system, the various cell lines expressing receptor mutants were stimulated with 100 nM phorbol myristate acetate to directly activate the luciferase reporter system.

Receptor Modeling. The template used for model building was an active conformation model of bovine rhodopsin (*10*) determined by applying experimentally derived distance restraints (from ligand binding, mutational, chemical labeling, and spectroscopic data) to the crystal structure of inactive bovine rhodopsin (PDB ID 1f88) (*9*). To construct a theoretical model of BLT_1, the amino acid sequences for the transmembrane regions of BLT_1 were aligned to the corresponding regions in the template according to Frimurer et al. (*18*).

Briefly, each transmembrane segment of the receptor was constructed using the template structure and the BLDPIR subroutine in WHAT IF (*19*). The loop regions of the receptor were then constructed using the DGINS option in WHAT IF. This is a best-fit method that selects loops from a database of crystal structures that match the sequence to be modeled (we used a series of overlapping loop sequence fragments). Loop template fragments were also interactively selected so that those residues overlapping the receptor residues adjacent to the loop should have an α-helical conformation. The introduction of defined secondary structure (such as sheets and helices) within the loops was avoided, and preference was given to loop fragments that had a "turn" or "coil" type of structure. Finally, fragments containing prolines were avoided unless there was a proline at the same location in the BLT_1 sequence. A highly conserved (within the GPCR superfamily) disulfide bond between Cys90 in the third transmembrane helix and Cys168 in the second extracellular loop was also included.

The resulting structure was then subjected to energy minimization "in vacuo", with torsional constraints applied to preserve the helices (to prevent helix unwinding and to mimic the lipid bilayer environment) using GROMOS87 [Van Gunsteren, W. F., and Berendsen, H. J. C. (1987) GROMOS: Groningen molecular simulation computer program package, University of Groningen, The Netherlands] as implemented in the WHAT IF software package. The final model was validated using the FULLCHK procedure in WHAT IF.

Ligand Docking. The ligand docking position was selected using two parallel strategies. The first approach used an iterative procedure that placed small probe atoms into the modeled active receptor in such a way as to minimize their interaction energies with the receptor protein, using the program PLIM [protein ligand interaction modeller (*20*)]. These probe atoms were given chemical characteristics similar to the various atoms in the ligand. The 10 best-fitting probes (lowest interaction energies) were selected within a given volume. This volume initially encompassed the entire membrane-spanning portion of the receptor but was subsequently reduced interactively.

The second approach utilized the program FlexX, version 1.10.1 (*21*), and the BLT_1 agonist, LTB_4. A virtual deprotonated LTB_4 molecule created using Sybyl (version 6.7.2; Tripos Inc., St. Louis, MO) was inserted by FlexX into a complete rigid model of BLT_1 in an active conformation. Free energy values were calculated for each of the FlexX-generated LTB_4 conformations, and the lowest energy conformations were selected for comparison with the PLIM probe atom positions.

Following docking, the LTB_4 conformation with the lowest energy was energy minimized in the absence of the receptor protein using the MMFF64s force field as implemented in Sybyl (version 6.7.2; Tripos Inc., St. Louis, MO), and this conformation was compared to the docked ligand structure. This was done to determine whether the docked ligand conformation was close to a local energy minimum.

Independent calculations, designed to detect cavities and caves in the receptor model, were also performed using WHAT IF in order to verify that the LTB_4 molecule had been docked into an accessible space large enough to accommodate it. This procedure was performed with the extracellular loops of the receptor in place and the same rigid receptor conformation used for docking.

Residues that could be important for ligand binding were identified using bioinformatic methods (Table 1) and by using WHAT IF to calculate the solvent (water) accessibility of the surface of the BLT_1 model. This latter procedure was performed with and without LTB_4 present (using the lowest energy conformation predicted by FlexX) in the proposed binding pocket to calculate the change in surface accessibility for each residue.

RESULTS

Ligand Conformations, Receptor Binding, and Efficacy. The efficacy of a series of substances structurally related to LTB_4 was determined to explore structure−activity relationships in the context of our experimental setup. For the following sections please refer to Figure 1 for molecular structures, which will be referred to below by the letters A−N.

The affinity of many ligands for BLT_1 is well documented. Our results, presented below and as Supporting Information, are in agreement with the bulk of the literature. The most

Table 1: Bioinformatic Identification of Ligand Binding Residues[a]

BLT_1 residue	accessibility change (Å²)[a]	highly conserved GPCR[b]	BLT_1/BLT_2 conserved[c]	BLT_1 conserved[d]	BLT_1 unique[e]
Val105	21.1		●	●	
Glu185	17.2		●	●	●
Met101	16.0		●	●	
Leu153	15.0			●	●
Arg178	12.5				●
Trp234	7.3		●	●	
Asn281	5.8	●	●	●	
Gly189	5.5			●	
Pro193	5.5	●	●	●	
Tyr102	4.7		●	●	●
His181	3.8		●	●	
Thr188	3.3		●	●	●
Phe230	2.8	●	●	●	
Ser277	2.4		●	●	
His94	1.9			●	●
Leu182	1.9		●	●	●
Gly98	1.6		●	●	●
Thr109	1.6		●	●	
Ile108	0.7			●	●
Tyr237	0.5			●	●
Ala274	0.4			●	●
Thr157	0.3				
Val158	0.3			●	●
Ser278	0.3			●	●

[a] Water accessibility to residues on the surface of BLT_1 was calculated before and after the addition of LTB_4 using the ACCESS subroutine in WHAT IF. BLT_1 residues with different accessibilities following ligand docking are ranked from the largest to the smallest change (in Å²). Residues shown in *italic* type were subsequently mutated. [b] Residues that are highly conserved within the rhodopsin receptor family. [c] LTB_4 binding residues identified by docking experiments that are also conserved in both BLT_1 and BLT_2. For this step BLT_1 (human, mouse, rat, guinea pig) and BLT_2 (human, mouse) isoform sequences were also aligned with four genetically related receptor sequences (human fMLP, c5a, somatostatin 2, and somatostatin 4 receptors). [d] Residues involved in LTB_4 binding conserved in BLT_1 isoforms. [e] The related receptor sequences (see footnote *c*) (but not BLT_2 isoforms) were used to eliminate BLT_1 residues that also occurred in genetically similar receptors and thus were probably conserved more generally. Most of the residues remaining after this procedure are also found in BLT_2.

potent ligand was found to be LTB_4, which had a mean EC_{50} value of 7.4 (1.7−12) nM (mean and 95% CI). The K_d for LTB_4 was determined to be 1.3 ± 0.5 nM (results are the mean ± SEM using triplicate measurements from three separate experiments). The B_{max} value calculated for receptor expression using data from the same experiments was 230 ± 20 fmol/mg of membrane protein. Under similar conditions, using membranes obtained from human granulocytes, LTB_4 competed for ^{3}H-LTB_4 membrane binding sites with a K_d of 1.7 ± 0.7 nM, and the calculated B_{max} value was 19 ± 2 fmol/mg of membrane protein, indicating that endogenous receptor expression in blood cell membranes is somewhat lower than in our recombinant cells.

Substances that were functionally inactive included various HETEs and prostaglandins, the cysteinyl leukotrienes LTC_4, LTD_4, and LTE_4, lipoxins A_4 and B_4, anandamide, arachidonic acid, 13*S*-HODE, and capsaicin (data not shown). No responses that were significantly different from experimental baselines were observed after administering these ligands to sham-transfected HF1 cells, with the exception of prostaglandin $F_2\alpha$, which had a stimulatory effect due to the endogenous expression of TP receptors by HeLa cells.

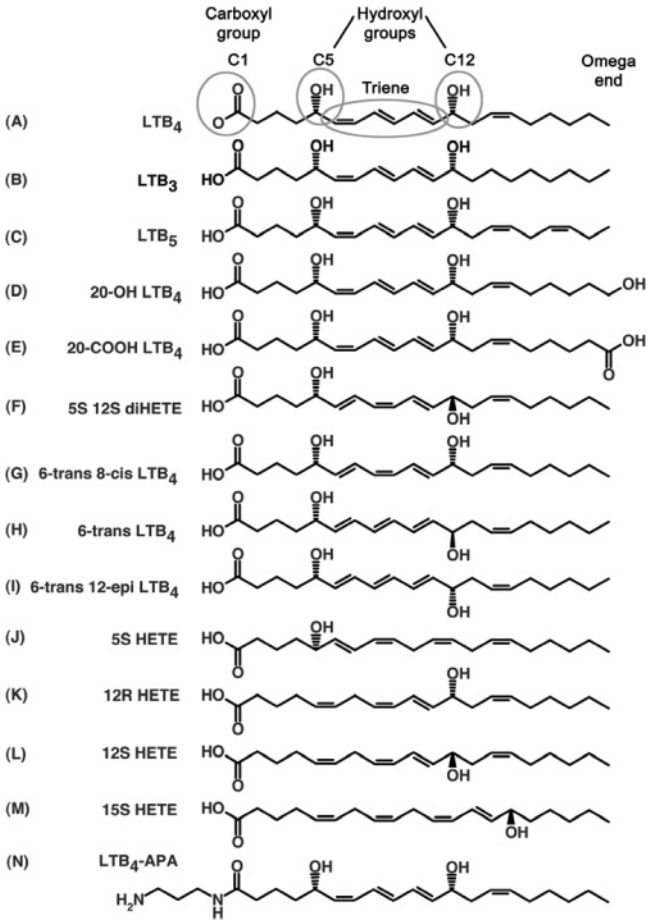

FIGURE 1: Leukotriene B_4 and structurally related eicosanoids.

Substances that were not active in functional assays were not tested using competition assays, with the exception of capsaicin. LTB_4 has been shown to bind to the capsaicin receptor VR1 (*22*), and so we determined whether there was a reciprocal interaction. Capsaicin was not, however, found to inhibit ^{3}H-LTB_4 binding to HeLa cell membranes expressing BLT_1 even at concentrations up to 40 μM.

The presence of the hydroxyl portion of the LTB_4 carboxyl group (which is deprotonated to produce the leukotriene's negative charge) is not essential for agonistic activity because if this group is replaced with aminopropylamine [as with LTB_4-APA (N)], the ligand is still active. Furthermore, after attaching the bulky fluorophore Alexa Fluor 568 to the free amino group on this molecule (*14*), the resulting ligand, LTB_4-568, could still bind to and activate the receptor.

Of the ligands we have studied, all of the most efficacious agonists had a C5 hydroxyl group in the *S* conformation. Several ligands, 12*R*-HETE (K), 12*S*-HETE (L), and 15*S*-HETE (M), lack a hydroxyl at this position. These ligands bind very poorly and have very low efficacies, with the exception of 12*R*-HETE, which is a weak agonist. Ligands such as 6-*trans*-LTB_4 (H), 6-*trans*-12-*epi*-LTB_4 (I), 5*S*,12*S*-diHETE (F), and, in particular, 5*S*-HETE (J), which have C5 hydroxyl groups in an appropriate conformation, also bind poorly, however, and have low efficacy.

Altering the configuration of the hydroxyl on the 12th carbon [as with 6-*trans*-12-*epi*-LTB_4 (I) or 5*S*,12*S*-diHETE (F)] produces molecules that bind very poorly to BLT_1. Similarly, 12*R*-HETE (K) binds to the receptor and retains some efficacy, whereas 12*S*-HETE (L) does not bind.

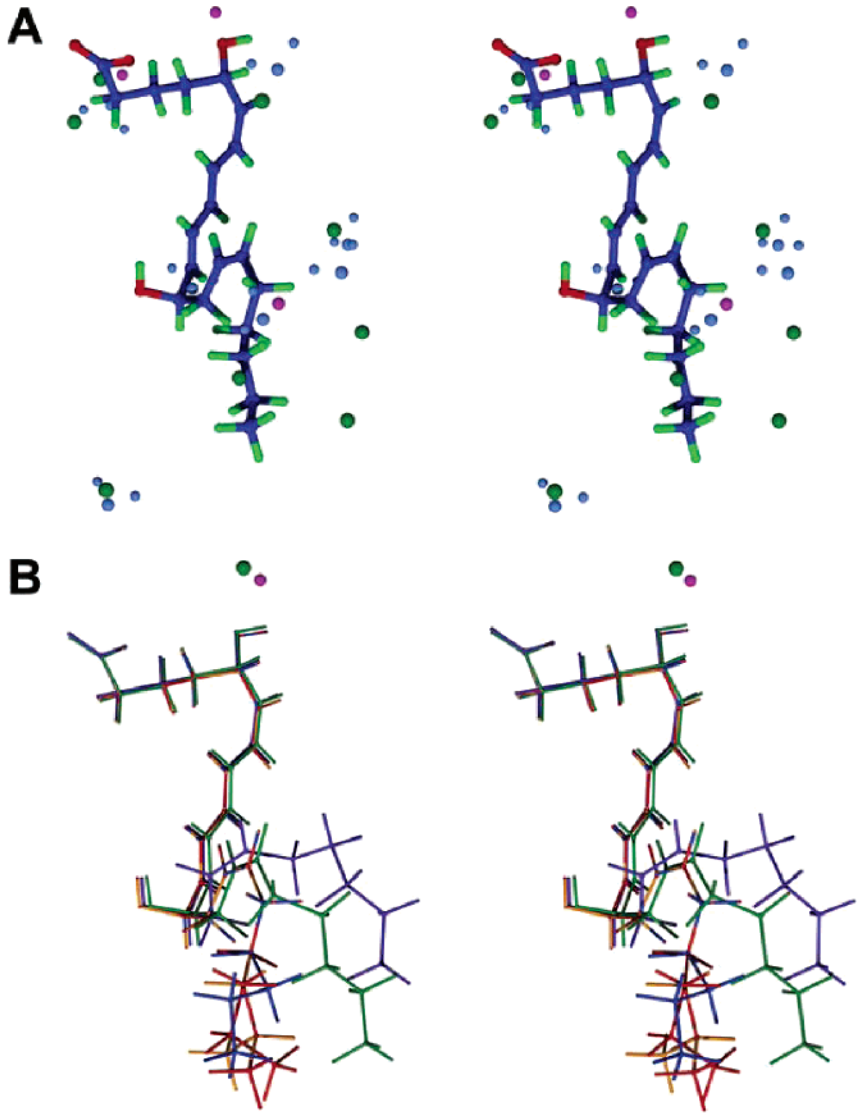

FIGURE 2: 3D computer models of BLT_1-bound LTB_4. (A) A defocused stereoview of PLIM probe atom positions is shown as multicolored spheres (blue for water, green for aliphatic carbons, and magenta for carboxylates). The lowest energy LTB_4 conformation proposed by FlexX is also shown as a ball and stick model (standard CPK colors). The C1 carboxyl is at the upper left, and the ω carbon C20 is at the bottom. (B) A defocused stereoview showing the conformations of the receptor-bound LTB_4 molecules with the lowest energies as determined by FlexX, colored from purple to red (highest to lowest energy). The receptor protein has been deleted for clarity.

Molecules lacking the C12 hydroxyl, such as 5*S*-HETE (J), bind very poorly and cannot activate BLT_1. If the hydroxyl group is moved to carbon 15, as with 15*S*-HETE (M), then binding is also reduced. Other substances, such as 13*S*-HODE, which lack the C5 and C12 hydroxylations, are completely inactive.

Adding a hydroxyl to the ligand at the ω carbon 20 (D) had very little effect on either ligand affinity for the receptor or ligand efficacy at the receptor. A more bulky and hydrophilic carboxyl group in this position produces a ligand [20-COOH-LTB_4 (E)] that binds to and activates the receptor less well.

Homology Modeling of BLT_1. There are several aspects of the receptor model that warrant comment. There are two probable glycosylation sites, Asp2 and Asp164, but we chose not to glycosylate the receptor given the uncertainties regarding the structure of possible glycosylations. In almost all GPCRs there is a highly conserved disulfide bridge that in BLT_1 connects Cys168 in the second extracellular loop and Cys90 in the third transmembrane helix, and our model was constructed with this constraint. Prolines occurring in the TM regions are also noteworthy because of the unusual geometry they can induce. There are seven prolines within the TM regions of BLT_1, and their locations are conserved in all BLT_1 and BLT_2 receptor isotypes. Only one of these, Pro72 in TM2, lacks representation in bovine rhodopsin. It is unlikely that the kinking in TM2 of BLT_1 resembles that of rhodopsin, because the Gly89-Gly90 sequence, and its position, in rhodopsin will cause the helix to kink differently than the Tyr70-Ala71-Pro72 motif in BLT_1. Most GPCRs are in fact very different to bovine rhodopsin in this region (*23*). A similar situation arises at the bottom of TM7 in BLT_1, where there are three glycines, and any deviation from normal helical geometry that may be caused by these glycines in BLT_1 was not present in the template structure and is thus not present in our model.

Ligand Docking. Only the membrane-spanning regions will be considered in detail with respect to ligand docking, and only those residues on TM3 and TM5 that we (or others) have investigated using point mutations will be dealt with

in detail. The extra- and intracellular loops may affect ligand binding, and they were present during docking, but the loop structures and their effect on the shape of the binding pocket remain speculative (although loop structures are based on conformations known to exist in crystallized proteins). The effects that the extracellular BLT_1 loops have on ligand binding will, however, remain unclear until more biochemical data emerge.

The BLT_1 agonist, LTB_4, was inserted in its deprotonated form into the rigid model of the active BLT_1 receptor using the FlexX (*21*) and PLIM (*20*) programs together, by first docking LTB_4 using FlexX and then comparing the resulting ligand conformations and positions with probe atom positions calculated using PLIM (Figure 2A). The two LTB_4 hydroxyl groups were docked in the vicinity of water probes and the carboxyl group near a carboxylate recognition site. Most probe atom positions that did not colocate with ligand atoms were in positions inaccessible to ligand atoms because of steric hindrance from surrounding atoms or were too deep down in the receptor to be accessible to ligands such as LTB_4. Some of the water molecule probes could also be in the ligand binding pocket even when the ligand is present. Taken together, the PLIM results overlap the ligand binding positions and conformations proposed by FlexX and support the proposed docking position.

To examine the binding of an agonist molecule (LTB_4) to BLT_1, we have used a computed model of the active conformation for rhodopsin (*10*) as a template for the construction of the BLT_1 model. Using FlexX, we initially attempted to dock LTB_4 into an inactive conformation of BLT_1 based on the rhodopsin crystal structure (*9*). While LTB_4 did bind, the lowest energy docking positions were found to be near the top of the receptor in a biologically implausible position, with the docked LTB_4 pointing out into the surrounding membrane lipids.

In the model presented here, the three LTB_4 conformations with the lowest energies covered a range of only 0.7 kcal/mol. The more extreme docking conformations of the LTB_4 molecule (the two outliers in Figure 2B) had energies differing by as much as 9.9 kcal/mol from the three lowest energy conformations. The ligand energy in a vacuum, as determined using the MMFF64s force field, was 8.4 kcal/mol. Using the lowest energy docking conformation of LTB_4, the ligand energy (when docked in the receptor) was calculated to be 12.9 kcal/mol. When the docked ligand conformation was energy minimized in the absence of the receptor protein, its energy fell only slightly to 11.7 kcal/mol. This indicates that this conformation corresponds to a local minimum close to the global minimum in vacuo. When bound to the receptor, this LTB_4 conformation is probably at a global minimum in that context.

The double bond conformation we have used for the triene portion of the docked ligand has been proposed following nuclear magnetic resonance studies of an LTB_4 potassium salt in an aqueous solution (*24*). Banères et al. (*8*) have proposed that the triene may be skewed, although the exact conformation is unknown. The triene portion of the lowest energy LTB_4 docking conformation in our active BLT_1 model is twisted by only 0.6 deg between the first double bond and the second and −3.1 deg between the second and the third.

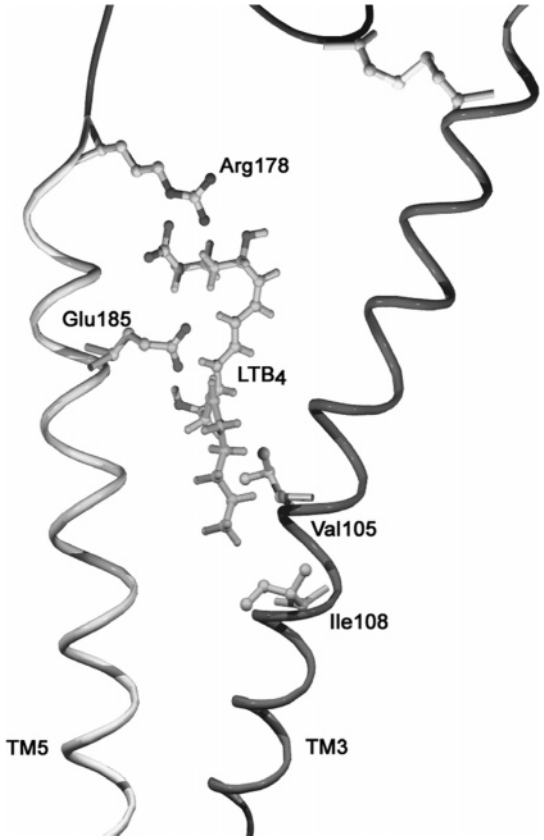

FIGURE 3: Ligand−receptor interactions. An overview of mutated residues in the BLT_1 binding cavity. For clarity, only part of extracellular loop 2, TM3, and TM5 are shown. The cysteine bridge between extracellular loop 2 (Cys168) and TM3 (Cys90) is visible at the top right of the figure. Not shown is Tyr237 from TM6.

To further support the proposed ligand position and structure within the receptor, we calculated the locations of cavities within the BLT_1 receptor. There is one large pocket in the receptor model; approximately 23 Å deep and 8 Å wide, this pocket is located between TM helices 3, 5, 6, and 7, and both FlexX and PLIM docked LTB_4 into this volume.

Following virtual LTB_4 docking, changes in the solvent accessibility (evaluated using water as a probe molecule) to the receptor surface indicated a number of residues that may be involved in ligand binding (Table 1). Almost all of the identified residues are conserved in BLT_1 isoforms, the exception being Arg178, which is represented by a similarly charged lysine in all other species for which the BLT_1 sequence is known. Most of the residues identified in this way are also conserved in BLT_2, and most are unique to the BLT_1/BLT_2 family if the amino acid sequences of genetically similar receptors are used to eliminate residues that are homologous in receptors that do not bind LTB_4.

BLT_1 Mutations: Effects on Receptor Function and Ligand Binding. An overview of most of our BLT_1 modifications is shown in Figure 3. All of the mutant BLT_1 receptors were expressed on the cell surface in varying amounts (Table 2), and almost all responded to LTB_4 stimulation (Tables 3−7), with the exception of the Val105Asp, Ile108His, and Ile108Asn mutations, which were almost inactive. Wild-type receptors C-terminally tagged with EGFP expressed well and were just as sensitive to LTB_4 (similar EC_{50}) as untagged receptors but did not signal as well in response to a given concentration (Table 3 and Figure 4). This attenuation of

Table 2: Radioligand Binding and Receptor Expression Data

cell line	$K_d \pm$ SEM (nM)[a]	*p*-value vs WT EGFP	B_{max} (fmol/mg)	expression (% of receptors on surface)[b]
sham	ND	ND	ND	1.3
wild type	1.3 ± 0.5	NS	230	96 (3.5)
WT EGFP	2.1 ± 0.4	ND	250	93
Arg178Glu	13 ± 1.5	<0.05	130	52
Arg178Leu	45 ± 3	<0.05	160	73
Glu185Val	64 ± 4	<0.05	175	81
Glu185His	32 ± 5	<0.05	105	55
Ile108His	ND	ND	ND	18
Ile108Asn	1.8 ± 1.5	NS	160	58
Val105Asp	38 ± 5	<0.05	105	39
Val105Thr	1.5 ± 1.8	NS	90	40
Tyr237Phe	2.5 ± 2.8	NS	170	71

[a] The affinity constants for ^{3}H-LTB_4 were obtained from saturation experiments using cell membrane fractions from cell lines expressing WT BLT_1 and various BLT_1 mutants. Data shown are the mean from duplicate wells in three separate experiments. NS = not significant; ND = not determined. [b] Receptor expression examined using a monoclonal anti-BLT_1 antibody. EGFP-tagged receptors are detected anywhere in the cell, whereas the antibody detects only those on the cell surface. The results are presented as the ratio of the total receptor number (the geometric mean of the EGFP fluorescence) to the number of receptors detected on the cell surface (the geometric mean of the BLT_1 antibody fluorescence). 100% represents only surface expression; 0% represents only intracellular expression. Antibody binding to untagged wild-type BLT_1 receptors is shown as the absolute proportion of cells labeled (isotype control labeling is shown in parentheses).

receptor signaling was observed for all of the mutants, except Arg178Glu (Table 4), which produced signals similar in magnitude to the untagged wild-type BLT_1 even though this mutant was less sensitive to LTB_4. The effect of various point mutations on the affinity of BLT_1 for LTB_4 and other ligands was also investigated (Tables 4−7), and in most cases affinity changes agree with the trends observed in the functional experiments such that decreased ligand binding is associated with decreased receptor activation. Ile108Asn (Table 6) and Val105Thr (Table 7) were exceptions. Membrane fractions expressing these mutants bound LTB_4 relatively well, but LTB_4 did not activate these mutants (using whole cells). The Tyr237Phe mutation on TM6 had no effect on ligand binding or receptor activation.

DISCUSSION

Previously Described BLT_1 Mutations. The work of Gearing et al. (*6*) with an epitope-tagged chimeric protein consisting of the extracellular half of BLT_1 and the intracellular half of the purine receptor, P2Y2, corroborates our proposed BLT_1 model. Some of the ligand binding residues that appeared to be involved in LTB_4 binding during virtual docking experiments are found within the BLT_1 regions that Gearing et al. replaced with the P2Y2 sequence, but most of these residues (Val105, Ile108, Thr109, Phe230), with the exception of Asn281, are represented by the same or similar amino acids in the P2Y2 receptor (isoleucine, leucine, threonine, and phenylalanine, respectively). The highly conserved Asn281 (from the TM7 NPXXY motif) is present in the proposed LTB_4 binding pocket, but this residue is probably not essential for ligand binding or receptor signaling because BLT_1/P2Y2 chimeric receptors with an aspartic acid at this point respond normally to LTB_4 (*6*). The cysteine-free BLT_1 receptor, produced by Banères et al. (*8*) by mutating all receptor cysteines (except Cys90 and 168) to serine, showed that cysteines are not involved in ligand binding (although they are necessary for structural integrity). We have also shown that the receptor is not sensitive to the sulfhydryl redox state of the extracellular medium (*25*). Later work by Mesnier and Banères (*26*) demonstrated that a Cys97Ser mutation did, however, have an effect on ligand binding affinity, so the importance of the cysteines on the extracellular surface remains unclear.

The Positive Charge at Arginine 178. The arginine residue at position 178 in BLT_1 (Figure 5) is important for ligand binding according to our mutational data and docking experiments. Reversing the Arg178 charge by inserting a glutamic acid did reduce LTB_4 binding affinity, as expected from the virtual model (Table 4). Removing the charge by mutating arginine 178 to a leucine further reduced the receptor affinity for LTB_4 (Figure 5). This suggests that, rather than charge interactions, there is a hydrogen-bonding network with LTB_4 that is partially maintained by the Arg178Glu mutant but not by the Arg178Leu mutant. There is a degree of flexibility in terms of which arginine and LTB_4 rotamers exist when LTB_4 is bound, but given the angles between the atoms involved in possible hydrogen bonds, it is possible that Arg178 can hydrogen bond to either the carboxyl group or the C5 hydroxyl of LTB_4. Other residues (notably the BLT_1/BLT_2 conserved His181) could also participate, but this remains speculative.

The relatively small change in ligand affinity when changing the charge of Arg178 is reversed was unexpected,

Table 3: LTB_4 Displacement and Signaling Using Wild-Type and Tagged Receptors

	ligand binding (competition assay)[a]			function (luciferase assay)[c]		
cell line	ligand	$K_i \pm$ SEM (nM)[b]	*p*-value vs WT EGFP K_i	$EC_{50} \pm$ SEM (nM)[d]	*p*-value vs WT EGFP EC_{50}	response range[e] (% WT) mean ± SEM
sham	LTB_4	ND[f]	ND	ND	ND	4.2 ± 0.4
wild type	LTB_4	1.7 ± 0.6	NS[f]	7.4 ± 1.5	<0.05	100
WT EGFP	LTB_4	3.1 ± 0.6	ND	13 ± 3	ND	32 ± 6

[a] The affinity constants for various ligands obtained from competition experiments using ^{3}H-LTB_4 and cell membrane fractions from cell lines expressing WT BLT_1 and various BLT_1 mutants. [b] The K_i values were determined by allowing test substances to compete for ^{3}H-LTB_4 binding sites (0.5 nM ^{3}H-LTB_4). Data shown are the mean from duplicate wells in three separate experiments. [c] Data obtained from luciferase reporter cell lines expressing WT BLT_1 and various BLT_1 mutants following stimulation with LTB_4 and various similar ligands. [d] EC_{50} values were determined following curve fitting quadruplicate concentration response curves from four separate experiments. Log EC_{50} values from each mutant were then compared using one-way ANOVA (with Bartlett's test for equal variances), and individual mutants were subsequently compared with wild-type EGFP-tagged receptors using Bonferroni's multiple comparison test. [e] The response range (fold change in luciferase activity) for each mutant was calculated as the response to the largest dose minus the response to the smallest dose using data from individual ($n = 16$) curve fits. Response ranges were then normalized using phorbol myristate acetate stimulation (see Experimental Procedures) and receptor expression levels. The maximum response of WT BLT_1 receptors was defined as 100%. [f] NS = not significant; ND = not determined.

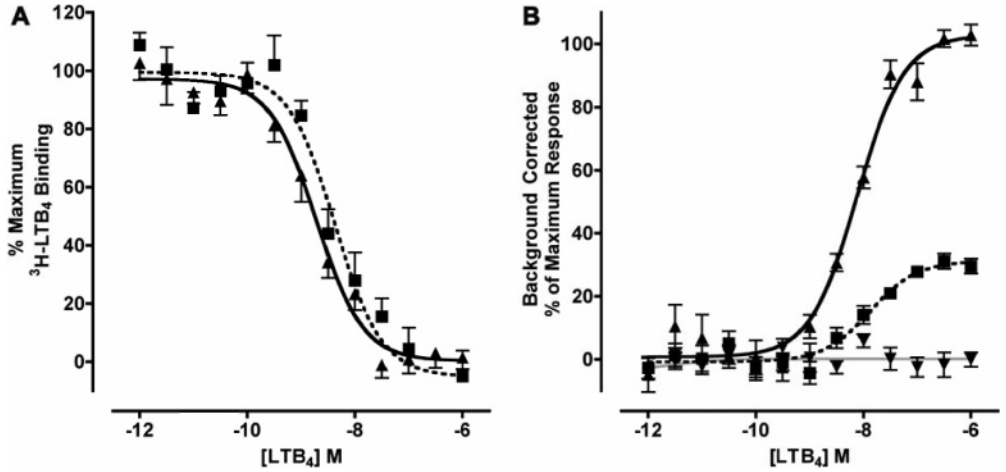

FIGURE 4: Competition binding and luciferase reporter gene expression for wild-type and EGFP-tagged BLT_1. (A) Displacement of 0.5 nM ^{3}H-LTB_4 binding to cell membrane preparations using increasing concentrations of unlabeled LTB_4. (▲ and solid line) WT BLT_1; (■ and dashed line) EGFP-tagged BLT_1. Data are shown as the mean ± SEM from duplicate wells in three separate experiments. (B) Luminescence following the expression of a luciferase reporter gene in response to increasing concentrations of LTB_4. Symbols as in panel A plus (▼ and solid gray line) sham-transfected control cells. Data are shown as the mean ± SEM from quadruplicate wells in four separate experiments.

Table 4: LTB_4 Displacement and Signaling Using Arg178 Mutants and C1 Modified Ligands[a]

	ligand binding (competition assay)			function (luciferase assay)		
cell line	ligand	K_i ± SEM (nM)	*p*-value vs WT EGFP K_i	EC_{50} ± SEM (nM)	*p*-value vs WT EGFP EC_{50}	response range (% WT) mean ± SEM
WT EGFP	LTB_4	3.1 ± 0.6	ND	13 ± 3	ND	32 ± 6
	LTB_4-APA	70 ± 4	ND	115 ± 20	ND	30 ± 7
	LTB_4-568	19 ± 2	ND	70 ± 13	ND	28 ± 6
Arg178Glu	LTB_4	16 ± 2	<0.05	40 ± 7	<0.05	100 ± 18
	LTB_4-APA	63 ± 6	NS	ND	ND	ND
	LTB_4-568	24 ± 3	NS	ND	ND	ND
Arg178Leu	LTB_4	41 ± 6	<0.05	47 ± 10	<0.05	47 ± 5
	LTB_4-APA	107 ± 13	NS	ND	ND	ND
	LTB_4-568	69 ± 12	<0.05	ND	ND	ND

[a] For an explanation of table headings see Table 3.

Table 5: LTB_4 Displacement and Signaling Using Glu185 Mutants[a]

	ligand binding (competition assay)			function (luciferase assay)		
cell line	ligand	K_i ± SEM (nM)	*p*-value vs WT EGFP K_i	EC_{50} ± SEM (nM)	*p*-value vs WT EGFP EC_{50}	response range (% WT) mean ± SEM
WT EGFP	LTB_4	3.1 ± 0.6	ND	13 ± 3	ND	32 ± 6
Glu185Val	LTB_4	58 ± 7	<0.05	81 ± 12	<0.001	24 ± 3
Glu185His	LTB_4	30 ± 5	<0.05	75 ± 7	<0.001	23 ± 3

[a] For an explanation of table headings see Table 3.

Table 6: LTB_4 Displacement and Signaling Using Val105 Mutants and C12 Modified Ligands[a]

	ligand binding (competition assay)			function (luciferase assay)		
cell line	ligand	K_i ± SEM (nM)	*p*-value vs WT EGFP K_i	EC_{50} ± SEM (nM)	*p*-value vs WT EGFP EC_{50}	response range (% WT) mean ± SEM
WT EGFP	LTB_4	3.1 ± 0.6	ND	13 ± 3	ND	32 ± 6
	12*S*-HETE	>1000	ND	>1000	ND	ND
Val105Asp	LTB_4	42 ± 5	<0.05	ND	ND	0.3 ± 0.15
	12*S*-HETE	>1000	ND	ND	ND	ND
Val105Thr	LTB_4	1.6 ± 1.5	NS	28 ± 3	NS	21 ± 3
	12*S*-HETE	>1000	ND	ND	ND	ND

[a] For an explanation of table headings see Table 3.

but we propose that this can be explained by considering the nature of the LTB_4 ligand and that there are precedents from studies using similar ligands (see below).

The presence of the hydroxyl portion of the LTB_4 carboxyl group (which is deprotonated to produce the leukotriene's negative charge) is not essential for agonistic activity, and even bulky fluorophores can be attached to this end of the ligand without destroying efficacy (*14*). While this implies that this end of the ligand is at the top of the binding pocket (because the bulky fluorophore is too large to bind further

Table 7: LTB_4 Displacement and Signaling Using Ile108 Mutants and C20 Modified Ligands[a]

	ligand binding (competition assay)			function (luciferase assay)		
cell line	ligand	$K_i \pm$ SEM (nM)	*p*-value vs WT EGFP K_i	$EC_{50} \pm$ SEM (nM)	*p*-value vs WT EGFP EC_{50}	response range (% WT) mean ± SEM
WT EGFP	LTB_4	3.1 ± 0.6	ND	13 ± 3	ND	32 ± 6
	20-OH-LTB_4	8.9 ± 2.1	ND	14 ± 5	ND	23 ± 4
	20-COOH-LTB_4	16 ± 2	ND	530 ± 60	ND	ND
Ile108His	LTB_4	ND	ND	ND	ND	7.1 ± 0.9
Ile108Asn	LTB_4	1.7 ± 2.1	NS	ND	ND	5.7 ± 0.9
	20-OH-LTB_4	5.2 ± 2.0	NS	ND	ND	ND
	20-COOH-LTB_4	11 ± 2	<0.05	ND	ND	ND

[a] For an explanation of table headings see Table 3.

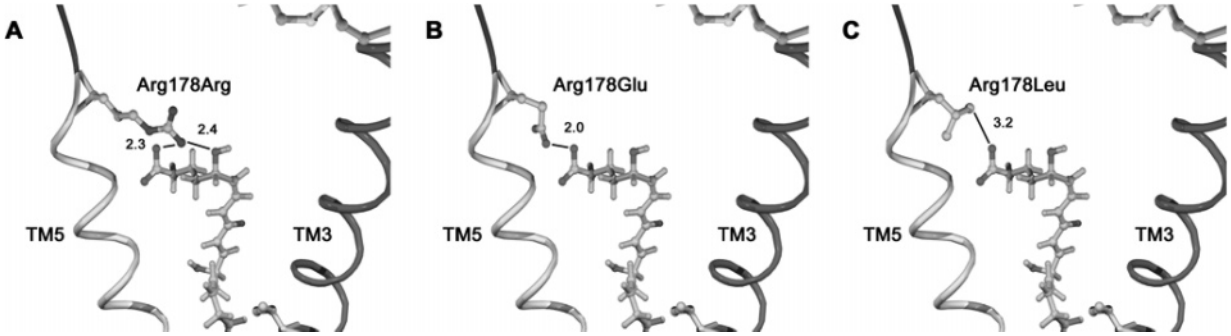

FIGURE 5: Arg178 mutations. For clarity, only part of extracellular loop 2, TM3, and TM5 are shown. The cysteine bridge between extracellular loop 2 (Cys168) and TM3 (Cys90) is visible at the top right in each frame of the figure. Distances are shown in angstroms but should be considered to be approximate.

down in the receptor), it also means the negative charge and an intact hydroxyl group bound to the first carbon atom are not critical for receptor activation. Ligands lacking this hydroxyl group do not, however, work as well as unmodified LTB_4, implying that at least part of the interaction occurs via this ligand epitope. To further investigate the nature of the receptor−ligand interaction, at this point we performed ligand binding experiments using LTB_4-APA and LTB_4-568 as ligands for WT, Arg178Glu, and Arg178Leu receptors (Table 4). We found that LTB_4, and ligands lacking the α-carbon hydroxyl, bound to these mutants in similar ways, implying that interactions between Arg178 and these ligands do not depend exclusively on the presence of the hydroxyl group on the first carbon and that hydrogen bonding rather than a salt bridge is likely responsible for ligand binding at this site.

The Arg178Glu mutant could also rescue the attenuated signal produced by EGFP-tagged BLT_1 such that this mutant signaled as well as untagged wild-type receptors. The reasons for this are not clear, and our data do not provide any insight. The Arg178 residue is on the extracellular surface of the ligand binding pocket at the top of TM5, the GPCR transmembrane helix that is least conserved and most often involved in ligand binding. Mutations in this helix could conceivably affect the concerted motions of the other helices, thus affecting the ability of the receptor to signal. The fact that only 50% of these mutated receptors make it to the cell surface also suggests that the receptor proteins might be missfolded and/or less stable, which might make it easier to shift them into an active state, but this is speculation.

Our modeling and mutational data suggested that, in addition to the interaction with the ligand carboxyl group, an interaction between Arg178 and the 5*S*-hydroxyl group of LTB_4 is also important. All of the most efficacious BLT_1 agonists had a C5 hydroxyl group in the *S* conformation, and the Arg178Glu mutant would still be able to participate in a hydrogen-bonding network with the C5 hydroxyl, whereas this would not occur when using the Arg178Leu mutant. Given that 12*R*-HETE (K) can also activate BLT_1, it seems that the 5*S*-hydroxyl cannot by itself stabilize the active receptor conformation and that activation of the receptor likely depends on interactions with other parts of the LTB_4 agonist as well. The interpretation of ligand efficacy data is, however, complicated by the fact that receptor ligands may induce distinct receptor conformations that favor one signaling pathway over another (*27*).

Results similar to ours have been reported using receptors for two other types of receptors for lipid ligands: the cannibinoid receptor, with the transmembrane 3 lysine mutated to glutamic acid, and the prostanoid receptors, with the highly conserved lysine from transmembrane 7 mutated to glutamic acid (*28*, *29*). Arginines are often utilized when anionic molecules must be docked into enzymes (*30*). LTA_4 hydrolase, the enzyme that synthesizes LTB_4 from its precursor molecule, has an active site reminiscent of the BLT_1 binding pocket, where an arginine and a lysine occupy the top of the pocket immediately adjacent to the substrate carboxyl group (*31*, *32*). A comparable arrangement has also been proposed for the binding of cysteinyl leukotrienes to the CysLT1 receptor (*33*). Only two of the BLT_1 surface arginines are conserved in BLT_2, and there is an uncharged alanine at the same position as Arg178 in BLT_1. This may explain the lower affinity of BLT_2 for LTB_4 as well as other eicosanoid ligands. Of the remaining BLT_1 arginines, most should not participate in ligand binding because they are positioned incorrectly, at least according to our data and computer model. An exception is Arg267, which is also conserved in BLT_2 and points into the binding pocket. Given

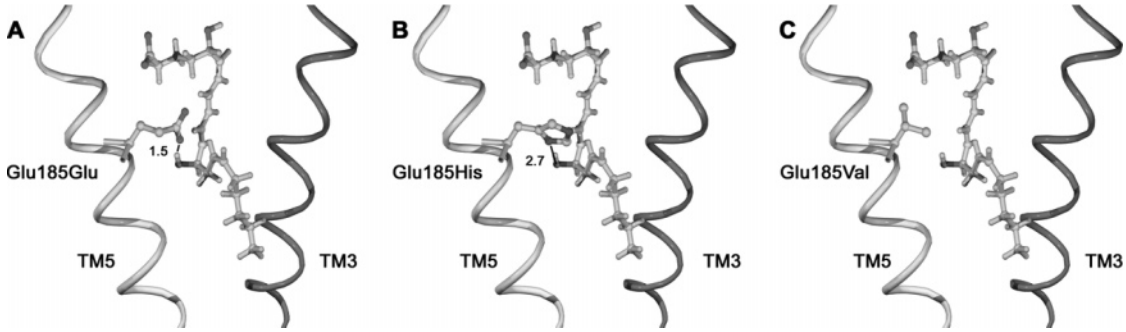

FIGURE 6: Glu185 mutations. For clarity, only TM3 and TM5 are shown. Approximate distances are shown in angstroms.

that our mutational data support the location we have proposed for LTB_4 binding, Arg267 is too far up for any interaction to occur with LTB_4, assuming that our model is correct for this part of TM7 (this is more likely than not, but this has not been tested).

TM6 and Tyrosine 237. It is also interesting to consider the Tyr237Phe mutation in the context of the discussion concerning Arg178 because the Tyr237Phe mutation had no effect on ligand binding or receptor signaling. Tyr237 is at the top of TM6, and modeling work suggested that this residue might be near the ligand carboxyl group, and we reasoned that it might also be important for stabilizing TM6 in an active conformation by participating in a hydrogen-bonding network involving the tyrosine hydroxyl group and the ligand carboxyl. The lack of effect that the removal of the tyrosine hydroxyl had on ligand binding suggests that this moiety is too distant to participate effectively in ligand binding.

Ligand Interactions with Glutamic Acid 185. Like the ligand binding to Arg178, the interactions between the ligand and Glu185 probably help to stabilize TM5 in its active conformation. The LTB_4 C12 hydroxyl group lies close to Glu185 in our model (Figure 6). Reversing the Glu185 charge using the Glu185His mutant reduced ligand affinity and efficacy (Table 5), and removing the possibilities for hydrogen bonding by mutating Glu185 to Val caused further reductions. Altering or removing the C12 hydroxyl (e.g., I, F, K, L, J, M) produced molecules that bind very poorly to BLT_1, so interactions between the ligand and the receptor at this point are also important. These interactions are not by themselves sufficient for complete receptor activation, however, so interactions with several residues on TM5 seem to be necessary to stabilize the active receptor conformation.

The Lower Portions of the BLT_1 Binding Pocket. To investigate how the tail portion of LTB_4 penetrated into the ligand binding pocket of the receptor, we mutated Val105 on TM5 (Figure 3). Modeling suggested that a large part of this residue's surface area was in contact with the receptor-bound LTB_4, and mutation of this residue to the more hydrophilic aspartic acid had a large effect on BLT_1 affinity for LTB_4, and this mutant did not signal (Table 6). Mutation of Val105 to the similarly sized but slightly more hydrophilic threonine had almost no effect on LTB_4 binding but did affect receptor signaling. Replacing Val105 with the slightly larger but hydrophobic isoleucine has previously been shown to have no effect on ligand binding or efficacy (*6*). These results are consistent with the hydrophobic tail portion of the leukotriene passing Val105.

Finally, we attempted to make the bottom of the binding pocket more polar by mutating Ile108 on TM3 (Figure 3) to asparagine or histidine. The Ile108His mutant did not express well (Table 7). The lower portions of the transmembrane part of the receptor are hydrophobic and tightly packed, so introducing this positively charged residue may disrupt receptor function after misfolding during expression. The more conservative Ile108Asn mutation, which introduces a polar side chain into the bottom of the binding pocket, bound LTB_4 normally and 20-COOH-LTB_4 (E) slightly better than WT BLT_1. While Ile108 is probably not very exposed to LTB_4, this supports the hypothesis that the ω carbon of LTB_4 probably extends down into this part of BLT_1. This mutant receptor did not signal, however.

Two other ligands of interest in this context are LTB_5 (C), which has a double bond in the *cis* conformation between C17 and C18, and LTB_3 (B), which lacks double bonds in the tail portion of the molecule. The addition of a double bond in LTB_5 reduces both ligand affinity and efficacy, and we propose that the more rigid tail structure probably does not fit well into the constricted bottom of the binding pocket. LTB_3, which has a completely saturated carbon tail, is almost a full agonist at BLT_1.

Mutational work by other groups also supports the binding position proposed in the present work, with the ligand tail extending downward into this part of the receptor. Trp234, in TM6, is positioned close to the LTB_4 tail in our model (near C15 to C18). This residue has been mutated by Banères et al. (*8*) to a leucine, which had no effect on LTB_4 binding, or to an alanine, which reduced receptor affinity for LTB_4. Maintaining a constricted hydrophobic environment in the bottom half of the binding pocket may therefore be important. Cysteine scanning of the lower half of TM6 also indicated that the presence of LTB_4 in the binding pocket would block access to Phe230 (*8*), which is also in agreement with our model.

Why Is BLT_1 More Selective Than BLT_2? The second leukotriene B_4 receptor, BLT_2, binds a larger range of ligands, including eicosanoids with C12 hydroxyl groups in the *S* conformation (*34*). The interactions, between relevant BLT_1 residues and the C12 hydroxyl groups of some leukotriene-like ligands, do not, however, help to explain why this would be. The residues involved (such as Glu185 and Val105 on TM3, mentioned above) are present in both BLT_1 and BLT_2, so it is not obvious from the present BLT_1 model or the BLT_2 sequence information why 12*S* eicosanoids bind with higher affinity to BLT_2. We mutated Val105 to threonine, a residue of similar size that has a hydroxyl group available for

hydrogen bonding to 12*S* ligands, and this did not have any effect on either BLT_1 affinity for LTB_4 or the efficacy of LTB_4 and did not enhance 12*S* binding (Table 6). Replacing Val105 with aspartic acid produced a receptor with much lower affinity for LTB_4 and no affinity for 12*R*-HETE or 12*S*-HETE (even though this mutant was expressed on the cell surface). So, the rejection of 12*S* ligands by BLT_1 does not seem to involve Val105. Both 12*R*- and 12*S*-HETE have different triene conformations from LTB_4, however, and this may prevent interactions between the C12 hydroxyls and this part of the receptor. It is also possible that BLT_2 has a significantly different binding mode from BLT_1. Recent work by Iizuka et al. (*35*) has revealed a BLT_2-specific agonist that, because of the size and chemical properties of this molecule, supports this idea.

CONCLUSIONS

We propose that LTB_4 binds in a pocket formed in the BLT_1 receptor by helices 3, 5, 6, and 7, with the polar carboxylate group of LTB_4 near the top of the pocket. The carboxylate group and the two hydroxyls of LTB_4 interact with Arg178 and Glu185 from transmembrane helix 5. Residues from transmembrane helix 3, Val105 and Ile108, also line the pocket further down in the receptor. We hope this work will be useful for the design of new more potent and more selective BLT_1 antagonists, as well as additional leukotriene receptor models.

ACKNOWLEDGMENT

We thank Dr. Knut Kotarsky for creating the HF1pBLT1 cells used in this study, Fredrik Tholander for assistance with some calculations, and Biolipox AB, Sweden, for access to their MicroBeta scintillation counter.

SUPPORTING INFORMATION AVAILABLE

(1) One table of the PCR primers used to create the BLT1-EGFP mutants. (2) Affinity and efficacy ranking of BLT_1 ligands. The competition constants for various leukotrienes and leukotriene-like substances at the human WT BLT_1 receptor as expressed in HF1pBLT1 cells are listed, and the ligands are ranked from highest to lowest affinity. The ligands are also ranked using mean EC_{50} values, obtained using the HF1pBLT1 luciferase reporter assay to measure WT BLT_1 activation following exposure to each ligand in the context of our experimental system. This material is available free of charge via the Internet at http://pubs.acs.org.

REFERENCES

1. Fretland, D. J., Gokhale, R., Mathur, L., Baron, D. A., Paulson, S. K., and Stolzenbach, J. (1995) Dermal inflammation in primates, mice, and guinea pigs: attenuation by second-generation leukotriene B4 receptor antagonist, SC-53228, *Inflammation 19*, 333−346.
2. Frieri, M., Therattil, J. M., Zitt, M., Bouboulis, D., Wang, S. F., Lark, G., Schaefer, P. A., and Sansone, G. (1998) Allergen-stimulated leukotriene B4 and interleukin-8 levels in patients with asthma and allergic rhinitis-modulation by a lipid pathway inhibitor, *Ann. Allergy Asthma Immunol. 81*, 331−336.
3. Aiello, R. J., Bourassa, P. A., Lindsey, S., Weng, W., Freeman, A., and Showell, H. J. (2002) Leukotriene B4 receptor antagonism reduces monocytic foam cells in mice, *Arterioscler. Thromb. Vasc. Biol. 22*, 443−449.
4. Griffiths, R. J., Pettipher, E. R., Koch, K., Farrell, C. A., Breslow, R., Conklyn, M. J., Smith, M. A., Hackman, B. C., Wimberly, D. J., Milici, A. J., et al. (1995) Leukotriene B4 plays a critical role in the progression of collagen-induced arthritis, *Proc. Natl. Acad. Sci. U.S.A. 92*, 517−521.
5. Chiang, N., Fierro, I. M., Gronert, K., and Serhan, C. N. (2000) Activation of lipoxin A(4) receptors by aspirin-triggered lipoxins and select peptides evokes ligand-specific responses in inflammation, *J. Exp. Med. 191*, 1197−1208.
6. Gearing, K. L., Barnes, A., Barnett, J., Brown, A., Cousens, D., Dowell, S., Green, A., Patel, K., Thomas, P., Volpe, F., and Marshall, F. (2003) Complex chimeras to map ligand binding sites of GPCRs, *Protein Eng. 16*, 365−372.
7. Baneres, J. L., and Parello, J. (2003) Structure-based analysis of GPCR function: evidence for a novel pentameric assembly between the dimeric leukotriene B4 receptor BLT1 and the G-protein, *J. Mol. Biol. 329*, 815−829.
8. Baneres, J. L., Martin, A., Hullot, P., Girard, J. P., Rossi, J. C., and Parello, J. (2003) Structure-based analysis of GPCR function: conformational adaptation of both agonist and receptor upon leukotriene B4 binding to recombinant BLT1, *J. Mol. Biol. 329*, 801−814.
9. Palczewski, K., Kumasaka, T., Hori, T., Behnke, C. A., Motoshima, H., Fox, B. A., Le Trong, I., Teller, D. C., Okada, T., Stenkamp, R. E., Yamamoto, M., and Miyano, M. (2000) Crystal structure of rhodopsin: A G protein-coupled receptor, *Science 289*, 739−745.
10. Gouldson, P. R., Kidley, N. J., Bywater, R. P., Psaroudakis, G., Brooks, H. D., Diaz, C., Shire, D., and Reynolds, C. A. (2004) Toward the active conformations of rhodopsin and the beta2-adrenergic receptor, *Proteins 56*, 67−84.
11. Mueller, M. J., Andberg, M. B., Samuelsson, B., and Haeggstrom, J. Z. (1996) Leukotriene A4 hydrolase, mutation of tyrosine 378 allows conversion of leukotriene A4 into an isomer of leukotriene B4, *J. Biol. Chem. 271*, 24345−24348.
12. Ollmann, I. R., Hogg, J. H., Munoz, B., Haeggström, J. Z., Samuelsson, B., and Wong, C.-H. (1995) Investigation of the inhibition of leukotriene A4 hydrolase, *Bioorg. Med. Chem. 3*, 969−995.
13. Stromberg, F., Hamberg, M., Rosenzvist, U., Dahlen, S. E., and Haegstrom, J. Z. (1996) Formation of a novel enzymatic metabolite of leukotriene A4 in tissues of *Xenopus laevis*, *Eur. J. Biochem. 238*, 599−605.
14. Sabirsh, A., Wetterholm, A., Bristulf, J., Leffler, H., Haeggstrom, J. Z., and Owman, C. (2005) Fluorescent leukotriene B4: potential application, *J. Lipid Res. 46*, 1339−1346.
15. Kotarsky, K., Owman, C., and Olde, B. (2001) A chimeric reporter gene allowing for clone selection and high-throughput screening of reporter cell lines expressing G-protein-coupled receptors, *Anal. Biochem. 288*, 209−215.
16. Sabirsh, A., Pettersson, A., Boketoft, A., Kotarsky, K., and Owman, C. (2003) Differential inhibition of receptor activation by two mouse monoclonal antibodies specific for the human leukotriene B4 receptor, BLT1, *Int. Immunopharmacol. 3*, 1829−1839.
17. Cheng, Y., and Prusoff, W. H. (1973) Relationship between the inhibition constant (K1) and the concentration of inhibitor which causes 50% inhibition (IC50) of an enzymatic reaction, *Biochem. Pharmacol. 22*, 3099−3108.
18. Frimurer, T. M., and Bywater, R. P. (1999) Structure of the integral membrane domain of the GLP1 receptor, *Proteins 35*, 375−386.
19. Vriend, G. (1990) WHAT IF: a molecular modeling and drug design program, *J. Mol. Graphics 8*, 29, 52−56.
20. Harris, M. R., Kihlen, M., and Bywater, R. P. (1993) PLIM−an automatic protein ligand interaction modeller, *J. Mol. Recognit. 6*, 111−115.
21. Kramer, B., Rarey, M., and Lengauer, T. (1999) Evaluation of the FLEXX incremental construction algorithm for protein-ligand docking, *Proteins 37*, 228−241.
22. Hwang, S. W., Cho, H., Kwak, J., Lee, S. Y., Kang, C. J., Jung, J., Cho, S., Min, K. H., Suh, Y. G., Kim, D., and Oh, U. (2000) Direct activation of capsaicin receptors by products of lipoxygenases: endogenous capsaicin-like substances, *Proc. Natl. Acad. Sci. U.S.A. 97*, 6155−6160.
23. Bywater, R. P. (2005) Location and nature of the residues important for ligand recognition in G-protein coupled receptors, *J. Mol. Recognit. 18*, 60−72.
24. Kingsbury, W. D., Pendrak, I., Leber, J. D., Boehm, J. C., Mallet, B., Sarau, H. M., Foley, J. J., Schmidt, D. B., and Daines, R. A.

(1993) Synthesis of structural analogs of leukotriene B4 and their receptor binding activity, *J. Med. Chem. 36*, 3308−3320.
25. Sabirsh, A., Bristulf, J., and Owman, C. (2004) Exploring the pharmacology of the leukotriene B4 receptor BLT1, without the confounding effects of BLT2, *Eur. J. Pharmacol. 499*, 53−65.
26. Mesnier, D., and Baneres, J. L. (2004) Cooperative conformational changes in a G-protein-coupled receptor dimer, the leukotriene B4 receptor BLT1, *J. Biol. Chem. 279*, 49664−49670.
27. Maudsley, S., Martin, B., and Luttrell, L. M. (2005) The origins of diversity and specificity in G protein-coupled receptor signaling, *J. Pharmacol. Exp. Ther. 314*, 485−494.
28. Chin, C. N., Murphy, J. W., Huffman, J. W., and Kendall, D. A. (1999) The third transmembrane helix of the cannabinoid receptor plays a role in the selectivity of aminoalkylindoles for CB2, peripheral cannabinoid receptor, *J. Pharmacol. Exp. Ther. 291*, 837−844.
29. Kedzie, K. M., Donello, J. E., Krauss, H. A., Regan, J. W., and Gil, D. W. (1998) A single amino-acid substitution in the EP2 prostaglandin receptor confers responsiveness to prostacyclin analogs, *Mol. Pharmacol. 54*, 584−590.
30. Riordan, J. F., McElvany, K. D., and Borders, C. L., Jr. (1977) Arginyl residues: anion recognition sites in enzymes, *Science 195*, 884−886.
31. Thunnissen, M. M., Nordlund, P., and Haeggstrom, J. Z. (2001) Crystal structure of human leukotriene A4 hydrolase, a bifunctional enzyme in inflammation, *Nat. Struct. Biol. 8*, 131−135.
32. Rudberg, P. C., Tholander, F., Andberg, M., Thunnissen, M. M., and Haeggstrom, J. Z. (2004) Leukotriene A4 hydrolase: identification of a common carboxylate recognition site for the epoxide hydrolase and aminopeptidase substrates, *J. Biol. Chem. 279*, 27376−27382.
33. Zwaagstra, M. E., Schoenmakers, S. H., Nederkoorn, P. H., Gelens, E., Timmerman, H., and Zhang, M. Q. (1998) Development of a three-dimensional CysLT1 (LTD4) antagonist model with an incorporated amino acid residue from the receptor, *J. Med. Chem. 41*, 1439−1445.
34. Yokomizo, T., Kato, K., Hagiya, H., Izumi, T., and Shimizu, T. (2001) Hydroxyeicosanoids bind to and activate the low affinity leukotriene B4 receptor, BLT2, *J. Biol. Chem. 276*, 12454−12459.
35. Iizuka, Y., Yokomizo, T., Terawaki, K., Komine, M., Tamaki, K., and Shimizu, T. (2005) Characterization of a mouse second leukotriene B4 receptor, mBLT2: BLT2-dependent ERK activation and cell migration of primary mouse keratinocytes, *J. Biol. Chem. 280*, 24816−24823.

BI060076T